Photogrammetric Brief

ARTHUR D. HOWARD
Stanford University
Stanford, Calif. 94305

Lunar Stereopairs

High-resolution photos were obtained during the Lunar Orbiter program.

ABSTRACT: *Lunar Orbiter vertical photographs taken in 1966 and 1967 have small areas of overlap. A number of stereopairs with scales ranging from approximately 1:7,000,000 to 1:35,000 have been prepared from this photography. Four examples are presented with brief discussion.*

INTRODUCTION

THE PRESENT NOTE was motivated by the excellent high-altitude oblique stereopair of the Aristarchus region of the Moon which appeared on the cover of the February issue of this journal. Although the stereopair had actually been set up pseudoscopically (see May issue, Erratum, page 499), the writer had no difficulty viewing it properly because of his familiarity with the topography of the area.

In a NASA report on possible lunar analogs of fluvial landscapes (Howard, Arthur, Lunar Analogs of Fluvial Landscapes: Possible Implications, NASA Report NGR-05-020-267, 95 p., Feb. 1970) a number of stereopairs illustrating lunar phenomena were presented. The stereopairs were prepared largely from high-resolution Lunar Orbiter IV photographs which cover the entire near face of the Moon and, to a lesser extent, from scattered photographs including medium resolution Lunar Orbiter IV and medium- and high-resolution Lunar Orbiter V photographs. The scales of these photographs varied because of changing altitude of the spacecraft. The scaler of the high-resolution Lunar Orbiter IV photos generally ranged between 1:600,000 and 1:700,000 whereas scales of the other photos used ranged from approximately 1:300,000 to as large as 1:35,000. Many of the photos have variable amount of overlap. Stereopairs of pertinent features of interest which happened to fall within the areas of overlap were prepared; four examples are herein. The relatively large scale of these vertical stereopairs contrasts with the extremely small scale of the February oblique cover illustration that is less than 1:2,000,000 in the central area. The larger scale reveals considerably more detail and makes possible refined interpretation. Although the primary purpose of this note is to present these examples of vertical stereopairs, a few comments on significant features and their possible interpretation are included.

THE STEREOPAIRS

Figure 1 is a view of Schroter's Valley, the prominent valley that appears in the February cover photograph. The viewer will undoubtedly be distracted by the apparent vertical offsets of the topography between adjacent horizontal strips (framelets). The offsets are due to the scanning, transmitting, and reassembly techniques employed in producing the photographs. Schroter's Valley starts in a crater, Cobra Head, on the northeast flank of the great crater Herodotus and continues some 80 miles (130 km) before terminating abruptly in a dead end. The inner rille, however, (Schroter's Rille) continues another 30 to 35 miles (48 to 56 km) eventually dying out on the surface of Oceanus Procellarum. The overall length of the rille, measured through the middle of the meander belt, is thus about 110 miles (180 km). The outer valley is interpreted as a graben whereas the appearance of the inner rille suggests erosion by a fluid agency. The two interruptions along the course of the rille in the lower part of the stereopair require explanation in the

fluid erosion hypothesis but these difficulties are not insurmountable. Disruption by meteorite impact or side slope deposition are among possible explanations. Single large-scale photos clearly indicate that side slope debris has crowded into the meanders where these hug the valley sides.

Figure 2 illustrates the Harbinger Mountains area just east of the Aristarchus Plateau. The area is off to the left of the February cover photograph. The large crater Prinz is shown in the upper left. The Harbinger Mountains, consisting of terra deposits of relatively high albedo, are surrounded by dark mare deposits identified elsewhere as basaltic in composition. Prinz Crater also antedates the more deposits that extend into its interior.

A variety of rilles are displayed. Rectilinear segments, the trends of which fall into regional sets, and the angular turns suggest fracture control of at least parts of several of the rilles. The evidence for fracture control is clear in the headward portions of most of the rilles but rectilinearity and angularity give way to sinuosity in the lower courses. A possi-

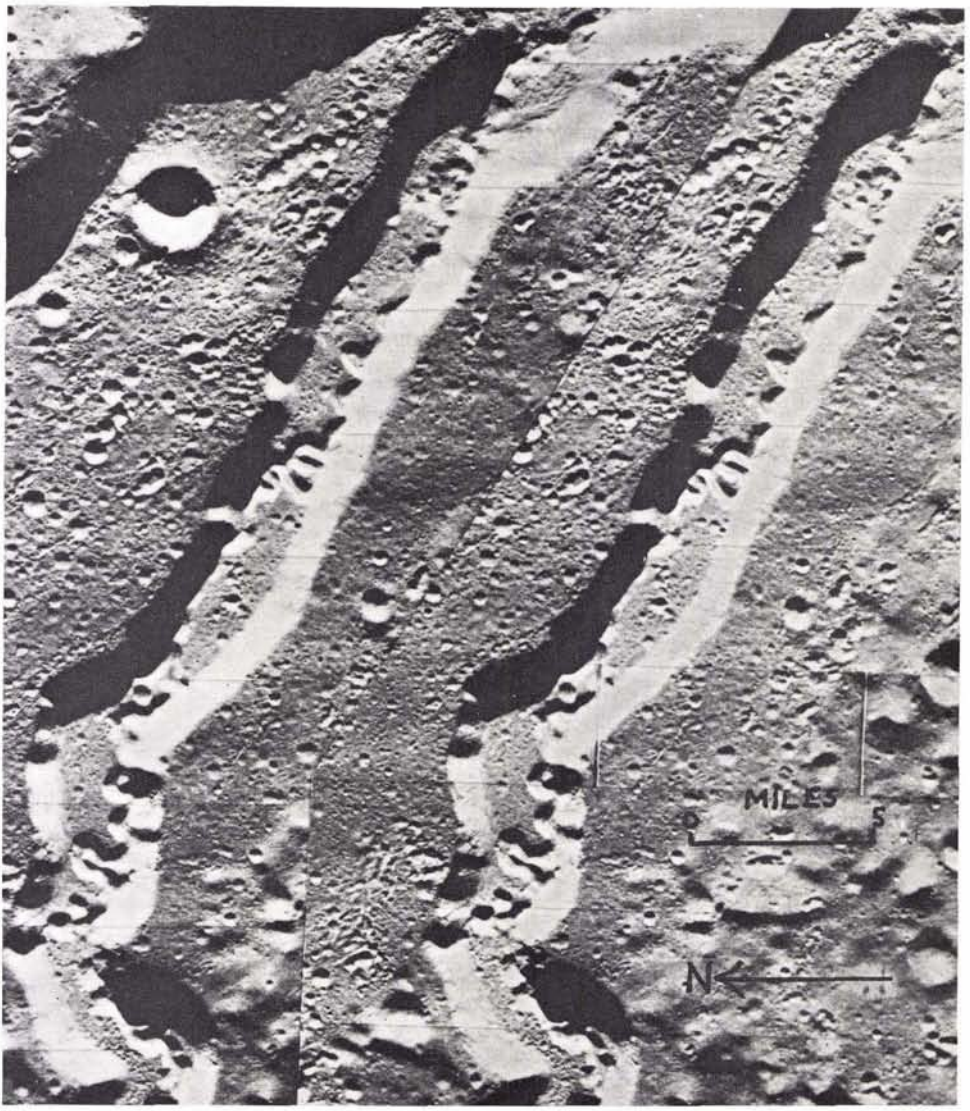

FIG. 1. Schroter's Valley and Schroter's Rille in the Aristarchus Plateau. Approximate coordinates: 26°N, 50°W. Stereopair prepared from high-resolution Lunar Orbiter V photos, frames 203 and 205. Date of photography; 18 August 1967.

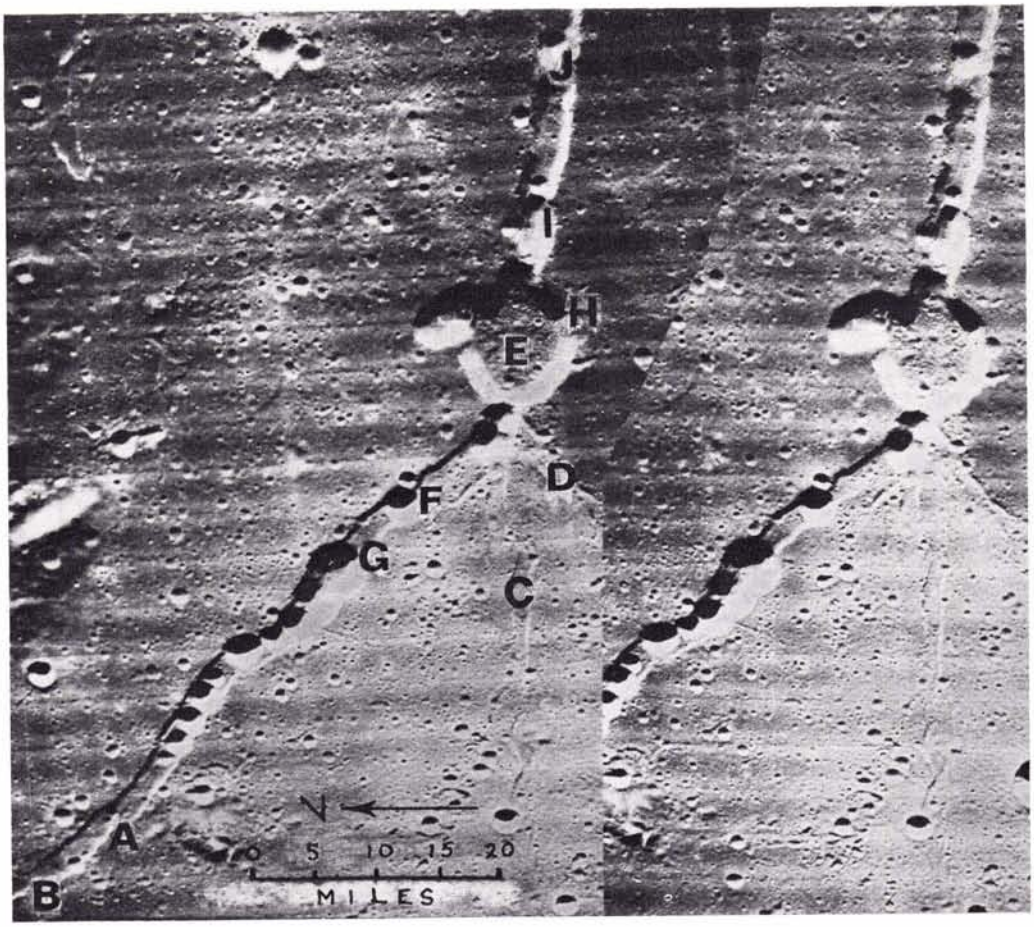
J
I
H
E
D
F
G
C
A
B
N
0 5 10 15 20
MILES

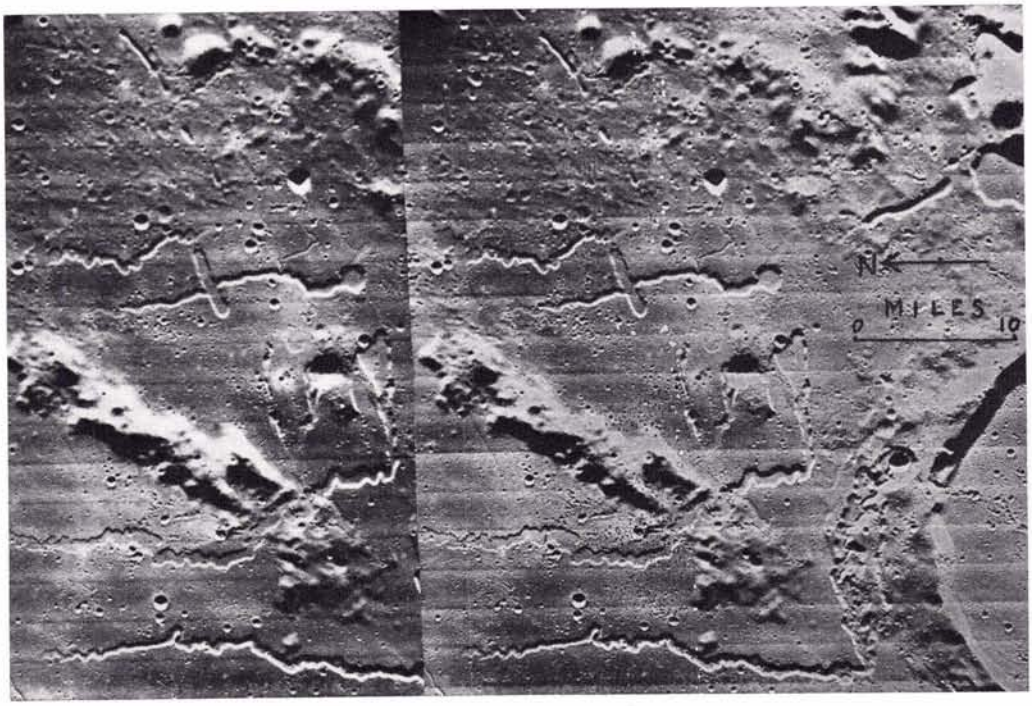
N
0 MILES 10

FIG. 2. Harbinger Mountains, east of Aristarchus Plateau. Approximate coordinates: 27°N, 43°W. Stereopair prepared from medium-resolution Lunar Orbiter V photos, frames 188 and 191. Data of photography: 18 August 1967.

ble explanation may be that fluids reached the surface by way of these fractures or graben-like depressions in the headward areas and developed sinuous courses away from the fracture zone. Note that the shortest of the four rilles, below the center of the model, has no depression at its head. Numerous such examples on the Moon argue against the suggested general explanation that sinuous rilles are eroded by internal fluids released at impact craters. The interrupted rectilinear rille in the lower part of the model parallels one of the major regional fracture trends and may indicate collapse along a reactivated subsurface fault. The rille that crosses the prominent ridge above the center of the model presents a unique problem. Superposition, antecedence, or piracy seem inadequate. It is more probable that a gap existed here similar to those between the hills in the lower part of the model. The gap could, of course, have been created by faulting. The spatula-like depression across the rille below the center of the model also parallels a regional fracture trend and is probably a graben. The fact that the downdropped segment of the rille is not shown on the graben floor suggests a subsequent fill.

Figure 3 is a view of Hyginus Rille, a generally recognized fracture feature. Note that in addition to the two main branches *EB* and *EJ* which extend from Hyginus Crater *E* there are other fainter fracture traces at *C* and *D*. The main branches are clearly graben with strings of craters of presumably internal origin. The craters are rimless as, for example, at *F* and *G*, but crater *I* is an exception. A small crater, *H*, indents the rim of Hyginus Crater. A remnant of the upland which failed to subside along the graben appears at *J*. A fault splinter and fault terrace are indicated at *A* and *B*, respectively.

Figure 4 is a view in the southern Apennines. The bold, linear, facetted escarpment overlooking Mare Imbrium in the upper left is almost certainly a fault scarp. Regional fractures in the hinterland are indicated not only by long lineaments (see arrows) but by the edentate crests of low ridges. A good example is shown along the east margin of the figure at the fourth framelet from the bottom. The most prominent fracture sets are northwest-southeast and northeast-southwest. Valleys seem to be integrated in some areas as indicated by the examples delineated in white. Many other examples, but on a much smaller scale, are detectable in the low hinterland areas.

FIG. 3. Hyginus Crater and Hyginus Rille. Approximate coordinates: 8°N, 6°W. Stereopair prepared from medium-resolution Lunar Orbiter V photos, frames 94 and 96. Date of photography: 14 August 1967.

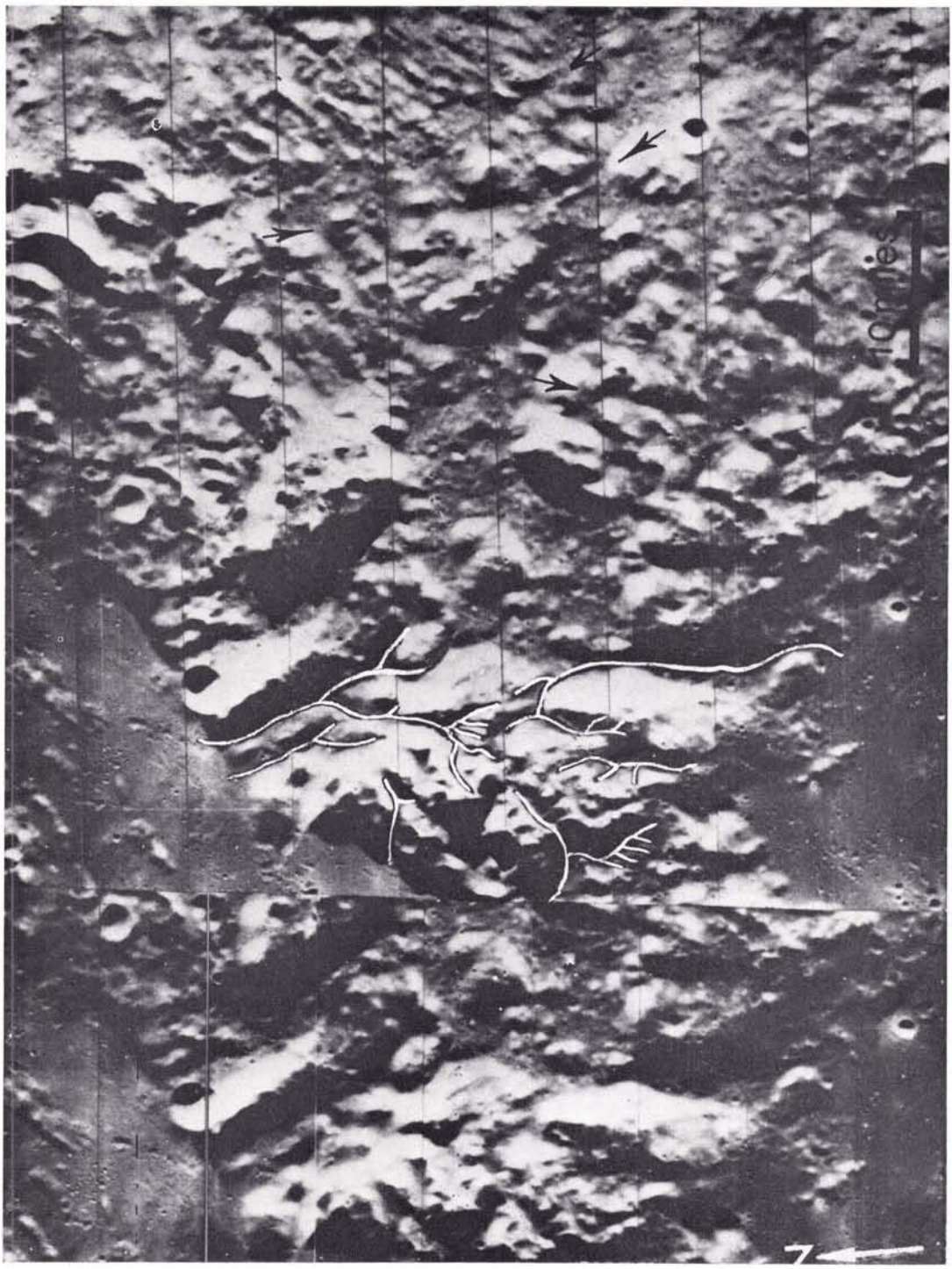

FIG. 4. Southern Apennine Mountains. Approximate coordinates: 17°N, 7°W. Stereopair prepared from high-resolution Lunar Orbiter IV photos, frames 109 and 114. Date of photography: 18–19 May 1967.